International Journal of Applied Electromagnetics and Mechanics 52 (2016) 1–6 1
IOS Press

Numerical Analysis of Quantum-Mechanical Non-uniform $\boldsymbol{E} \times \boldsymbol{B}$ Drift: Non-uniform electric field

Wataru Kosaka [a,*], Shun-ichi Oikawa [b] and Poh Kam Chan [a]

[a] *Graduate School of Engineering, Hokkaido University, Sapporo 060-8628, Japan*

[b] *Faculty of Engineering, Hokkaido University, Sapporo 060-8628, Japan*

Abstract. We have numerically solved the two-dimensional time-dependent Schrödinger equation for a charged particle in the presence of a non-uniform electric field $\boldsymbol{E} = E\,(1 - y/L_E)\,\boldsymbol{e}_y$ as well as a non-uniform magnetic field $\boldsymbol{B} = B\,(1 - y/L_B)\,\boldsymbol{e}_z$. It is shown that such a non-uniformity of the electric field does not affect the time rate of the variance, or uncertainty, changes in position and momentum, while that of the magnetic field does.

Kewords: Schrödinger equation, uncertainty, non-uniform magnetic field, non-uniform electric field, quantum mechanical effect, expansion rate, GPU parallel computing

1. Introduction

The charged particles drift in the presence of a magnetic field $\boldsymbol{B}$, the drifts include ∇B drift, curvature drift and $\boldsymbol{E} \times \boldsymbol{B}$ drift if there exist an electric field $\boldsymbol{E}$. The two-dimensional time-dependent Schrödinger equation have been already solved for a charged particle in the presence of a non-uniform magnetic field and a uniform electric field, in which it was shown that the variance, or the uncertainty, in position $\sigma_r^2\,(t)$ grows with time [1–5]. For the typical fusion plasma with a temperature $T \sim 10$ keV and a number density of $n \sim 10^{20}$ m^{-3}, the standard deviation $\sigma_r\,(t)$ would reach the interparticle separation $n^{-1/3}$ in a time interval of the order of 10^{-4} sec. After this time the wavefunctions of neighboring particles would overlap, as a result the conventional classical analysis may lose its validity [1]. In Ref. [1] mentioned above, the uniform electric field have been assumed. In this paper, quantum mechanical effects of a non-uniform electric field and a non-uniform magnetic field will be studied. In section 2, methods of numerical analysis of time-dependent Schrödinger equation is briefly described. In section 3, time evolution of the variances and their dependence on physical parameters, e.g. m, q, v_0, B, L_B, E, and L_E are shown. Section 4 summarizes the study.

2. Schödinger equation

The unsteady Schrödinger equation for wavefunction $\psi\,(\boldsymbol{r}, t)$, at a position $\boldsymbol{r}$ and a time t, is given by

*Corresponding author: Wataru Kosaka, Graduate School of Engineering, Hokkaido University, Sapporo 060-8628, Japan, E-mail: wataru_k@fusion.qe.eng.hokudai.ac.jp

$$i\hbar \frac{\partial \psi}{\partial t} = \left[\frac{1}{2m} \left(-i\hbar \nabla - q\boldsymbol{A} \right)^2 + qV \right] \psi, \tag{1}$$

where $V = V(\boldsymbol{r})$ and $\boldsymbol{A} = \boldsymbol{A}(\boldsymbol{r})$ stand for the scalar and vector potentials, m and q the mass and electric charge of the particle, and $i \equiv \sqrt{-1}$ the imaginary unit, $\hbar$ the reduced Planck constant.

2.1. Numerical analysis

In the Cartesian coordinate system (x, y, z), we assume the magnetic field $\boldsymbol{B} \parallel \boldsymbol{e}_z$ and the electric field $\boldsymbol{E} \perp \boldsymbol{e}_z$, where $\boldsymbol{e}_z$ is z-direction unit vector. In this case, the wavefunction $\psi(x, y, z, t)$ is decomposed into $\psi(x, y, t)$ which corresponds to cyclotron motion in x-y plane and $\psi(z, t)$ which corresponds to free particle motion in z-direction.

We will solve Eq. (1) with an appropriate initial condition in x-y plane, using the finite difference method (FDM) in space with the Crank-Nicolson scheme [1–5].

For the Crank-Nicolson scheme with the central difference method in space, partial differential equation Eq. (1) is reduced to the following matrix equation,

$$\left(\mathsf{I} - \frac{\Delta t}{2i\hbar} \mathsf{H} \right) \left\{ \psi^{n+1} \right\} = \left(\mathsf{I} + \frac{\Delta t}{2i\hbar} \mathsf{H} \right) \{ \psi^n \}. \tag{2}$$

Here, $\{\psi^n\}$ stands for the discretized wavefunction, the superscript n represents the time-label, I and H are the unit matrix and the numerical Hamiltonian matrix [1–5]. Assuming the Coulomb gauge $\nabla \cdot \boldsymbol{A} = 0$, the numerical Hamiltonian matrix $\mathsf{H} \equiv \left\{ H_{i,j} \right\}$ is written as follows,

$$H_{i,j} = \frac{1}{2m} \left[\nabla_{i,j}^2 + 2i\hbar q \boldsymbol{A}_{i,j} \cdot \nabla_{i,j} + \left(q\boldsymbol{A}_{i,j} \right)^2 \right] + qV_{i,j}, \tag{3}$$

where $\boldsymbol{A}_{i,j}$ and $\nabla_{i,j}$ represent the discretized operators, as

$$\nabla_{i,j}^2 \psi = \frac{\psi_{i-1,j} - 2\psi_{i,j} + \psi_{i+1,j}}{\Delta x^2} + \frac{\psi_{i,j-1} - 2\psi_{i,j} + \psi_{i,j+1}}{\Delta y^2}, \tag{4}$$

and the subscripts i and j represent x- and y- node numbers. Equations (2) and (3) are quadratic in accuracy over both the time step Δt and the grid size Δx and Δy.

The time integrator U is derived from Eq. (2) as,

$$\mathsf{U} \equiv \left(\mathsf{I} - \frac{\Delta t}{2i\hbar} \mathsf{H} \right)^{-1} \left(\mathsf{I} + \frac{\Delta t}{2i\hbar} \mathsf{H} \right). \tag{5}$$

It should be noted that the time integrator is not only unconditionally stable but also norm-conserving for discretized wavefunction $\{\psi\}$. The latter leads to the strict particle conservation, irrespective of Δt, Δx and Δy, since the matrix H is Hermitian, so that the matrix U is unitary; the Euclidean norm $\| \{\psi\} \|_2 =$ const with time [1].

We will also adopt the successive over relaxation (SOR) scheme for time integration in Eq. (2).

$$\left\{ \psi^{n+1} \right\}^{(k+1)} = \left\{ \psi^{n+1} \right\}^{(k)} + \omega_{\mathrm{SOR}} \{R\}^{(k)}, \tag{6}$$

where

$$\{R\} = \frac{1}{\alpha}\left[\{\phi^n\} - \left(\mathsf{I} - \frac{\Delta t}{2\mathrm{i}\hbar}\mathsf{H}\right)\left\{\psi^{n+1}\right\}\right], \tag{7}$$

$$\{\phi^n\} = \left(\mathsf{I} + \frac{\Delta t}{2\mathrm{i}\hbar}\mathsf{H}\right)\{\psi^n\}, \tag{8}$$

$\{R\}$ is the residual in Eq. (2), α stands for the diagonal element in LHS of Eq. (2), superscript (k) represents the number of iterations, ω_{SOR} is the relaxation factor and $\omega_{\mathrm{SOR}} = 1.01$ is adopted in this study. For the convergence criterion, we have used the following,

$$\frac{1}{N_x N_y}\sum_{i,j=1}^{N_x,N_y}\left|R_{i,j}\right|^2 \leq \epsilon_{\mathrm{SOR}}, \tag{9}$$

where N_x and N_y represent the number of nodes in x- and y-direction, and $\epsilon_{\mathrm{SOR}} = 5\times10^{-31}$ in this study.

Since Eq. (6) can be executed in parallel, we have used a graphics processing unit (GPU) [9] for this purpose.

3. Numerical results

In the numerical results to be presented in the following, physical parameters are normalized as; mass of the particle $m = m_p = 1.6722\times10^{-27}$ kg, charge $q = e = 1.602\times10^{-19}$ C, velocity $v = 10\,\mathrm{ms}^{-1}$ and magnetic field $B = 10\,\mathrm{T}$ [1]. Thus, normalization constants of length ρ, time t and electric field E are $\rho = m_p v/eB = 1.0438\times10^{-8}$ m, $t = m_p/eB = 1.0438\times10^{-9}$ s and $E = vB = 100\,\mathrm{Vm}^{-1}$. The Schrödinger equation is solved in the presence of a scalar potential of $qV = -qEy\,(1 - y/2L_E)$ and a vector potential of $q\boldsymbol{A} = -qBy\,(1 - y/2L_B)\,\boldsymbol{e}_y$, where L_E and L_B stand for a gradient scale length of a electric field and magnetic field.

When the corresponding classical particle has a canonical momentum $\boldsymbol{p}_0 = m\boldsymbol{v}_0 + q\boldsymbol{A}\,(\boldsymbol{r}_0)$, where $\boldsymbol{v}_0$ is the initial velocity at a position $\boldsymbol{r} = \boldsymbol{r}_0$, initially at a time $t = 0$, the initial condition for the wavefunction $\psi\,(\boldsymbol{r}, 0)$ can be given [6, 7] by

$$\psi(\boldsymbol{r}, 0) = \frac{1}{\sqrt{\pi}\sigma_B}\exp\left[-\frac{(\boldsymbol{r} - \boldsymbol{r}_0)^2}{2\sigma_B^2} + \mathrm{i}\boldsymbol{k}_0\cdot\boldsymbol{r}\right], \tag{10}$$

where $\boldsymbol{k}_0 = \boldsymbol{p}_0/\hbar$ is the initial wavenumber vector, and $\sigma_B \equiv \sqrt{\hbar/qB}$ is known as the magnetic length in quantum mechanics [8].

3.1. Numerical errors

There are three invariants of motion, the energy $\mathcal{E} = \left\langle\hat{H}\right\rangle$, the canonical momentum in x-direction $P_x = \langle -\mathrm{i}\hbar\partial/\partial x\rangle = \left\langle m\hat{v}_x - q\hat{A}_x\right\rangle$, since the potentials V and $\boldsymbol{A}$ do not depend on x, as well as particle conservation $\int_\Sigma |\psi|^2 \mathrm{d}S = 1$. Here, $\left\langle\hat{f}\right\rangle$ stands for the expectation value of an operator $\hat{f}$, i.e. $\left\langle\hat{f}\right\rangle = \int_\Sigma \psi^*\hat{f}\psi\,\mathrm{d}S$. The absolute numerical errors in these invariants are quite small as shown Fig. 1.

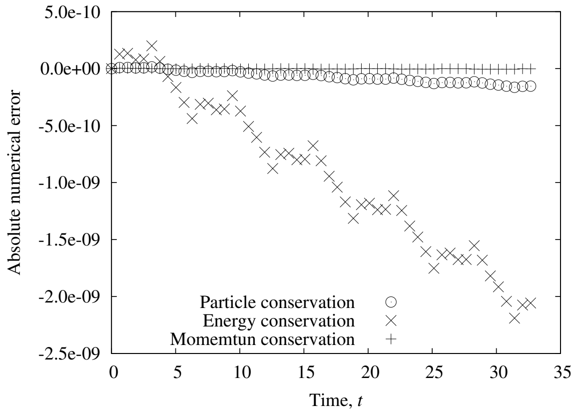

Fig. 1. Absolute errors for the invariants of a particle, energy and x-component of the canonical momentum for $q = m = B = 1$, $v_0 = 5$, $E = 10^{-3}$ and $L_E = L_B = 10^{-4}$. Their initial values are 1 (exact), ~5 and ~13.

3.2. Time evolution of variances

The time dependent variances in position $\sigma_r^2(t)$ and mechanical momentum $\sigma_{mv}^2(t)$ oscillate with each gyration period, such as $2\pi/\omega_c$ and π/ω_c, where ω_c is the cyclotron frequency, as shown Fig. 2. In both uniform and non-uniform conditions, the variances slightly grow with time. Since the exact variances should not grow with time in the presence of a uniform electromagnetic field, these time evolution $\sigma^2_{\mathrm{non-uniform}}(t)$ are due purely to numerical errors. On the other hand, the time evolution $\sigma^2_{\mathrm{uniform}}(t)$ in the presence of the non-uniform electromagnetic field consists of physical increment and about the same numerical errors as the case of the uniform field. Thus, let us define the increment of variances, $\Delta\sigma^2(t)$, between $\sigma^2_{\mathrm{non-uniform}}(t)$ and $\sigma^2_{\mathrm{uniform}}(t)$, as [1, 2]

$$\Delta\sigma^2(t) = \sigma^2_{\mathrm{non-uniform}}(t) - \sigma^2_{\mathrm{uniform}}(t)\,. \tag{11}$$

The increment $\Delta\sigma^2(t)$ shows the physical time evolution of variances, as shown in Fig. 3. Also depicted in the figure is a fitting line, which represents the time averaged evolution of variance. Let us also define the expansion rate in position $\mathrm{d}\sigma_r^2/\mathrm{d}t$ and mechanical momentum $\mathrm{d}\sigma_{mv}^2/\mathrm{d}t$, using the fitting lines' gradient.

3.3. Rate of changes in variances

For various combinations of physical parameters, such as m, q, v_0, E, B, L_B and L_E, similar analyses to that in the preceding section give us the relationship between the expansion rate of variances in position $\mathrm{d}\sigma_r^2(t)/\mathrm{d}t$ as a function of $\hbar v_0/qBL_B$, as shown in the left panel of Fig. 4, and in mechanical momentum $\mathrm{d}\sigma_{mv}^2(t)/\mathrm{d}t$ as a function of $\hbar qBv_0/L_B$ in the right panel of Fig. 4. Also depicted are the fitting lines. It is noted that the variances clearly on the respective fitting lines of

$$\frac{\mathrm{d}\sigma_r^2}{\mathrm{d}t} = (2.00 \pm 0.03)\,\frac{\hbar}{qB}\frac{v_0}{L_B}, \tag{12}$$

$$\frac{\mathrm{d}\sigma_{mv}^2}{\mathrm{d}t} = (1.030 \pm 0.005)\,\hbar qB\frac{v_0}{L_B}, \tag{13}$$

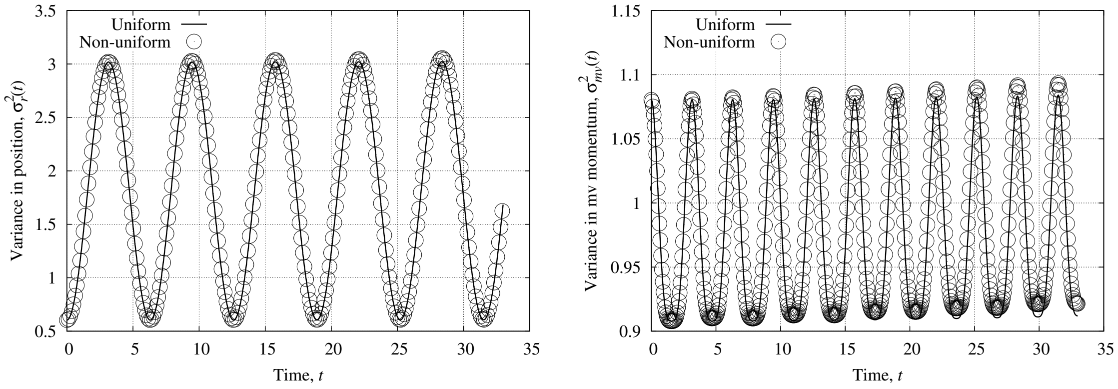

Fig. 2. Time evolution of variance in position $\sigma_r^2(t) = \left\langle \boldsymbol{r}^2 \right\rangle - \langle \boldsymbol{r} \rangle^2$ (left) and in mechanical momentum $\sigma_{mv}^2(t) = \left\langle (m\boldsymbol{v})^2 \right\rangle - \langle m\boldsymbol{v} \rangle^2$ (right), for initial velocity $v_0 = 5$, charge $q = 1$, mass $m = 1$, electric field $E = 10^{-3}$ with $L_E = 10^{-4}$, magnetic field $B = 1$, thus $\omega_c = 1$, with $L_B = 10^{-4}$ or ∞.

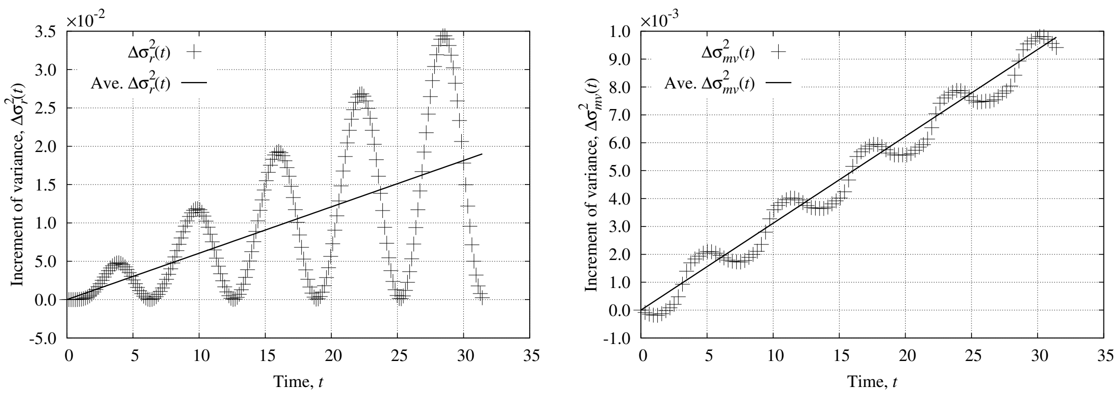

Fig. 3. Time evolution of increment of variance in position $\Delta\sigma_r^2(t)$ (left), and mechanical momentum $\Delta\sigma_{mv}^2(t)$ (right). Ave. $\Delta\sigma_r^2(t)$ and Ave. $\Delta\sigma_{mv}^2(t)$ stand for the time average over the cyclotron period, for the case presented in Fig. 2.

both of which do not depend on the particle mass m, the magnitude of electric field E nor the gradient scale length of electric field L_E. Therefore, it is shown that the non-uniform electric field $\boldsymbol{E} = E(1 - y/L_E)\,\boldsymbol{e}_y$ does not affect the expansion rates while the non-uniform magnetic field $\boldsymbol{B} = B(1 - y/L_B)\,\boldsymbol{e}_z$ does.

Let us apply the expansion rate to the typical fusion plasma with a temperature $T = 10\,\mathrm{keV}$, number density $n = 10^{20}\,\mathrm{m}^{-3}$, a magnetic field $B = 5\,\mathrm{T}$ and a gradient scale length of magnetic field $L_B = 3\,\mathrm{m}$, which is the major axis of a torus. When we take a proton for the charged particle and the thermal velocity $v_{\mathrm{th}} \sim 1.352 \times 10^6\,\mathrm{m/s}$ for v_0 in Eq. (13), the standard deviation $\sigma_r^2(t)$ of the proton reaches the interparticle separation $n^{-1/3}$ in a time interval 0.38 msec. In contrast, the ion-ion collision time is about 20 msec [10]. Thus, overlapping of wavefunctions of neighboring protons would occur before the conventional collision time.

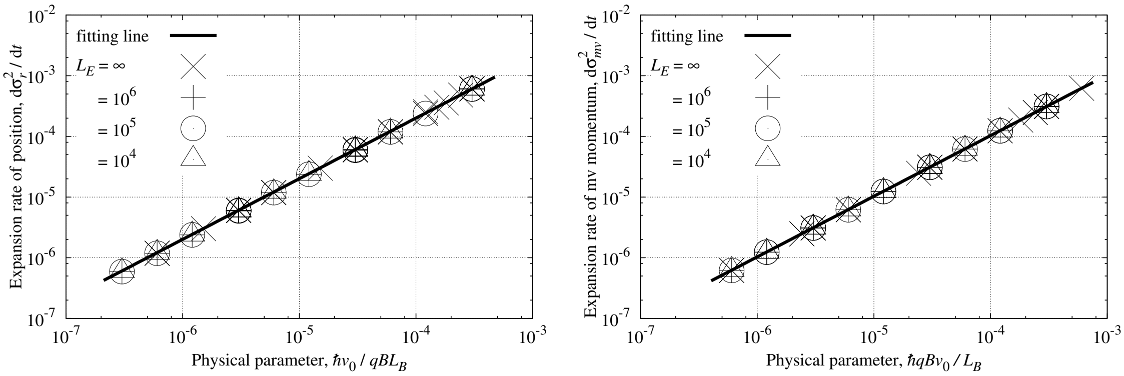

Fig. 4. Expansion rate of variance in position vs. $\hbar v_0/qBL_B$ (left) and in mechanical momentum vs. $\hbar qBv_0/L_B$ (right). Each point shape, such as ◇ and □, corresponds to the same gradient scale length of electric field L_E.

4. Summary

We have solved the two-dimensional time-dependent Schödinger equation for a charged particle in the presence of a non-uniform electric field $\boldsymbol{B} = B(1 - y/L_B)\, \boldsymbol{e}_z$ and magnetic field $\boldsymbol{E} = E\,(1 - y/L_E)\, \boldsymbol{e}_y$. It is shown that the particle mass and the electric field do not affect the expansion rate as long as the electric field has the uniform gradient.

Acknowledgments

The authors would like to thank Prof. S. Tomioka, Prof. Y. Matsumoto and Prof. Emeritus M. Itagaki for their fruitful discussions on the subject. Part of the SOR coding for a GPU was done by Dr. R. Ueda. This research was partially supported by a Grant-in-Aid for Scientific Research (C), Japan, 21560061.

References

[1] S. Oikawa, W. Kosaka and P. K. Chan, *Plasma Fusion Res.* **9**, 3401033 (2014).
[2] S. Oikawa, and P. K. Chan, Plasma Fusion Res. **8**, 2401142 (2013).
[3] P. K. Chan, S. Oikawa, and E. Okubo, Plasma Fusion Res. **7**, 2401034 (2012).
[4] S. Oikawa, E. Okubo, and P. K. Chan, Plasma Fusion Res. **7**, 2401106 (2012).
[5] S. Oikawa, T. Shimazaki, and E. Okubo, Plasma Fusion Res. **6**, 2401058 (2011).
[6] H. Natori and T. Munehisa, J. Phys. Soc. Jpn. **66**, pp. 351–359 (1997)
[7] J. J. Sakurai, *Modern Quantum Mechanics*, Rev. ed., (Addison-Wesley, Reading, 1994).
[8] L. D. Landau and E. M. Lifshitz, *Quantum Mechanics*: *Non-relativistic Theory*, 3rd ed., translated from the Russian by J. B. Sykes and J. S. Bell (Pergamon Press, Oxford, 1977).
[9] http://www.nvidia.com.
[10] J. D. Huba, "NRL PLASMA FORMULARY", Naval Research Laboratory, 2013.